ASTRONOMY
AND
ASTROPHYSICS

WR 121 obscured by a dust cloud: the key to understanding occasional "eclipses" of "dusty" Wolf-Rayet WC stars?[⋆]

P.M. Veen[1], A.M. van Genderen[1], K.A. van der Hucht[2], A. Li[1], C. Sterken[3][⋆⋆], and C. Dominik[1]

[1] Leiden Observatory, Postbox 9513, 2300 RA Leiden, The Netherlands
[2] Space Research Organization Netherlands, Sorbonnelaan 2, 3584 CA Utrecht, The Netherlands
[3] University of Brussels, Pleinlaan 2, B-1050 Brussels, Belgium

Abstract. We observed the Wolf-Rayet star WR 121 (= AS 320, WC9) coming out of a minimum with a depth of $0\overset{m}{.}8$ to its normal brightness in a dozen days. The nature of this event was analyzed by means of Walraven five-colour photometry. The colour changes are similar to those caused by interstellar dust. Hot dust is known to be formed continuously around this carbon-rich Wolf-Rayet star. Therefore, we suggest that the fading of WR 121 was caused by the temporary condensation of an optically thick line-of-sight dust cloud, comparable to what occurs around R Coronae Borealis stars.

We suggest that occasional "eclipses" shown by other "dusty" Wolf Rayet stars (WR 113, WR 103) are also caused by such temporary condensing dust clouds. In addition, we present observations of a new "eclipse" of WR 103. This brightness dip was more shallow than the earlier "eclipses" and the star reddens during the descent. This also supports the model of a condensing dust cloud.

From modeling the shapes of the various "eclipses" we find that the condensation takes place at radii ranging from 80 to 800 $R_\odot$, i.e. between the stellar surface and the permanent dust shell that is inferred from the infrared excess. From the colour changes we estimate the sizes of the particles in the clouds to be of order 0.1 μm and using the depth of the darkening we derive a dust mass condensation rate per column in the range of 3 – 20 10^{-10}kg m^{-2}s^{-1}. The dust mass flux per solid angle turns out to be comparable to that of the shell. Moreover, we find two possible trends within our small set of "eclipses": (1) the closer the condensation occurs to the star, the larger the dust mass flux is, and (2) the closer the condensation, the larger the particles are. These correlations are discussed within the framework of the model.

Key words: stars: Wolf-Rayet – stars: individual: WR 121, WR 103, WR 113 – circumstellar matter

1. Introduction

One of the many remarkable observations of Wolf-Rayet (WR) stars are the "eclipses" of a few carbon-rich late-type stars (WC8 and WC9), that can not be attributed to an observed companion, or to variability of the star itself. We consider it significant that all these objects happen to have an infrared excess due to circumstellar dust. The presence of dust shells around WC late-type stars is investigated by Williams et al. (1987, henceforth WHT) and reviewed by Williams (1995a). The classification of WC stars is quantified by Smith et al. (1990), abundances are quantified by Torres (1988), Smith & Hummer (1988) and Eenens & Williams (1992). Recently, a spectral analysis of WC5–7 stars, including one dust-less WC8 star, was presented by Koesterke & Hamann (1995). More general information on WR stars can be found in the catalogue by van der Hucht et al. (1981) and in the review by van der Hucht (1992).

We feel that in astronomy the word 'eclipse' means an occultation by a solid body. Therefore, we will call the shape of the light curve eclipse-like, a drop in brightness, a fading, or an "eclipse". The word "obscuration" will be used to indicate our interpretation of the observations as an occultation by a cloud.

In this paper, we present two new drops in brightness; one of WR 103 (HD 164270, WC 9), a star that has shown occasional "eclipses" before, and one of WR 121 (= AS 320, WC 9), a faint object for which no earlier "eclipses" were reported. The observations of the latter "eclipse" turned out to contain crucial information for the development of a model. Mind *Note added in proof*.

WR 121 was first noted as a Wolf-Rayet object by Merrill & Burwell (1950). The strong Hα emission-line on their objective-prism spectra, is presumably due to the He II λ6560 and C II λ6578 lines, since hydrogen lines were never observed later on (Torres & Massey 1987). Like most WC 9 stars, WR 121 shows a stable hot dust shell in the infrared survey by WHT. Stellar parameters were determined by Howarth & Schmutz (1992) by modeling near-infrared spectra. Furthermore, spectropolarimetry of WR 121 does not show lines (Schmidt 1988), indicating that the line emission and continuum are formed in a

Table 1. Catalog parameters of WR stars discussed in this paper and the comparison stars (C). The fourth and fifth columns list the Smith (1968) magnitudes or otherwise as indicated.

star	other designation	spectral type	v	$b - v$	reference
WR 103	HD 164270	WC9	$9^{\mathrm{m}}01$	$0^{\mathrm{m}}03$	van der Hucht et al. 1981
WR 113	CV Ser	WC9 + O8-9 III-V	$9^{\mathrm{m}}43$	$0^{\mathrm{m}}47$	van der Hucht et al. 1981
WR 121	AS 320	WC9	$12^{\mathrm{m}}43$	$0^{\mathrm{m}}95$	Lundström & Stenholm 1984
C 121	HD 174916	Am	$V_{\mathrm{J}} = 7^{\mathrm{m}}40$	$(B - V)_{\mathrm{J}} = 0^{\mathrm{m}}39$	Feinstein 1974, this paper
C 103	HD 164152	B9V	$y = 8^{\mathrm{m}}892$	$b - y = 0^{\mathrm{m}}06$	Sterken et al. 1993

Table 2. Observers of WR 121

Observer(s)	date		year
R. S. lePoole &	1/9	- 13/10	1989
R. A. Reijns			
R. van Ojik	18/6	- 3/7	1990
J. van Grunsven	24/7	- 29/7	1990
G. C. Fehmers	9/8	- 19/8	1990
A. M. Janssens	10/9	- 1/10	1990
M. J. Zijderveld	7/10	- 21/10	1990

spherically symmetric volume (Schulte-Ladbeck 1994). Table 1 lists the observational parameters of the stars mentioned above plus WR 113 (CV Ser, WC8 + O8-9 III-V), the first star for which an occasional "eclipse" was reported.

The next section discusses the reduction of the photometric observations of WR 121 and presents the resulting light- and colour curves. In Sect. 2.2 the new "eclipse" of WR 103 is presented. In Sect. 3 we discuss earlier "eclipses" and the models that have been applied rather unsuccessfully. Sect. 4 introduces the dust shells around late type WC stars. Sect. 5 describes the phenomenological model of a cloud condensing in the line of sight and the individual fits. The results will be interpreted and discussed in Sect. 6, and a connection will be made with the R Coronae Borealis (RCrB) stars. Sect. 7 will summarize the conclusions.

2. Observations of new obscurations

2.1. WR 121

2.1.1. Observations and reduction

The observations of WR 121 were obtained with the Dutch 90-cm telescope at La Silla (ESO, Chile) equipped with the simultaneous five-colour photometer of Walraven ($VBLUW$: λ_{eff} is 5441, 4298, 3837, 3623, and 3235 Å, respectively). The photometric system is described in detail by Lub & Pel (1977). The data were obtained by different observers as listed in Table 2. The observations of WR 121 were performed in cycles with the comparison star C = HD 174916 (Am) and another WR star WR 123 as follows: C–sky–121–123–C–121–123–C–sky, etc. The observations of WR 123 will not be discussed here. Inte-

gration times were 30 seconds for the comparison star and one minute for the program stars and the sky background.

Between the first run in 1989 and the ones in 1990 the observing strategy was changed, because in the first observing run there was too much scatter that could be ascribed to two very faint background stars. Therefore, the sky was measured at another position and found to be stable. Also a larger diaphragm was used, $21''5$ instead of $16''5$ to ensure that a nearby optical companion to WR 123 would always be inside the aperture. Because of this sky problem, the data set from 1989 was discarded in determining the mean photometric properties of the stars as listed in Table 3. Note that in the Walraven system the photometric parameters are in log intensity scale (i.e. magnitudes divided by -2.5); magnitudes will be indicated explicitly using superscript "m". Johnson filters are indicated with subscript J. For stars with normal spectra the Walraven log I scale can be transformed to the Johnson V_{J} and $(B - V)_{\mathrm{J}}$ with (Pel 1986):

$$V_{\mathrm{J}} = 6^{\mathrm{m}}886 - 2.5[V + 0.033(V - B)] \tag{1}$$

$$
\begin{aligned}
(B - V)_{\mathrm{J}} = {} & 2.571(V - B) - 1.020(V - B)^2 \\
& + 0.500(V - B)^3 - 0^{\mathrm{m}}010
\end{aligned} \tag{2}
$$

The calculated V_{J} and $(B - V)_{\mathrm{J}}$ values of HD 174916 are identical to the values measured by Feinstein (1974) (see Table 3).

The photometric quality of each night was judged using the large number of observations of other program and comparison stars. Furthermore, every single observation made by the Walraven photometer is split into two halves and the difference between these is an indication of the quality of the measurement. On this basis we rejected several data points.

Because of the faintness of the object the sky contributes considerably to the raw flux measurement, especially when the moon was nearby. We rejected measurements for which the sky contributed more than 60 % in the V-band and more than 75% in the B- L-, U-bands). All the data from the W-band were neglected because of the sky contribution.

2.1.2. Light- and colour curves

The differential light curves of WR 121 in Fig. 1 shows the fading of WR 121. Because HD 174916 is much brighter than WR 121, we reproduce here also the light curve of WR 123, as additional evidence that the observations are not in error. According to Moffat & Shara (1986), WR 123 is slightly variable
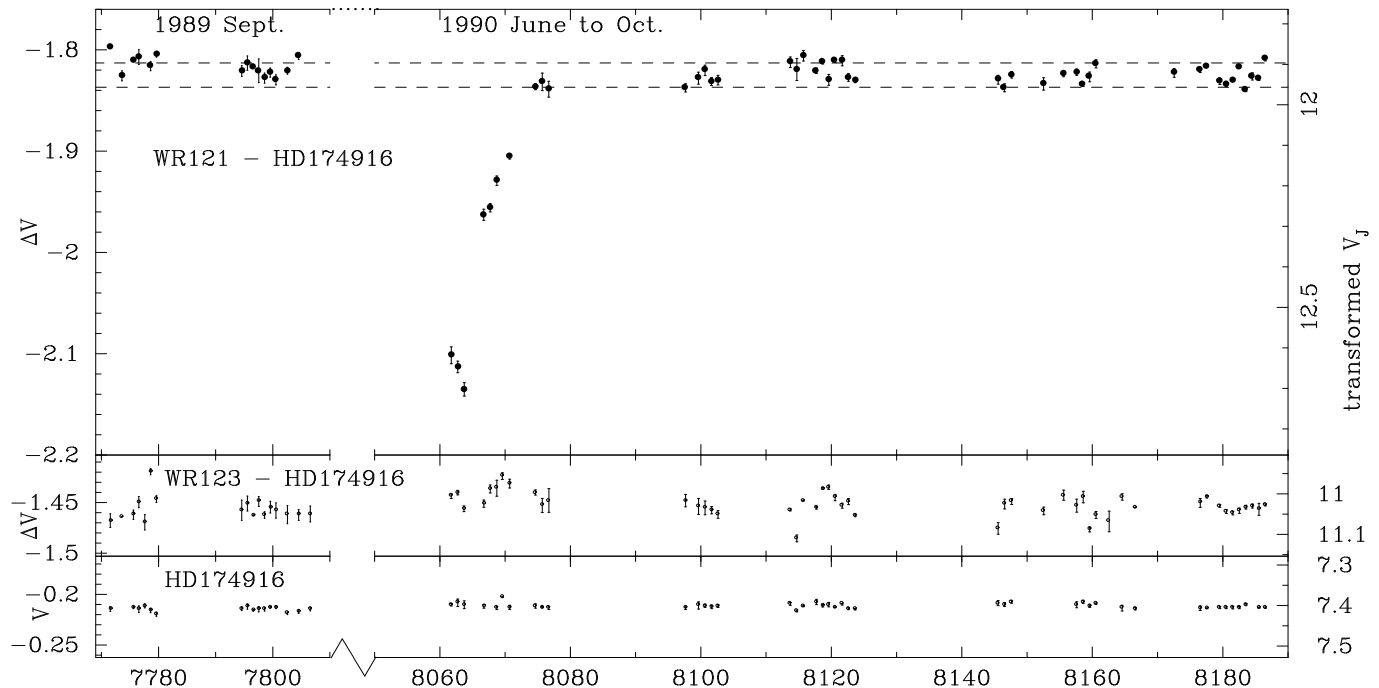
Fig. 1. The differential Walraven V photometry (magnitude scale on the right) of WR 121 is shown as a function of heliocentric Julian date together with that of WR 123 and the absolute photometry of the comparison star. The dashed lines represent the mean "after obscuration" value plus or minus three times the mean nightly standard deviation.

Table 3. Mean Walraven photometric parameters in log intensity scale of the comparison star (C = HD 174916) and of the program star WR 121 unobscured *relative to the comparison star*. The V_J and $(B - V)_J$ values are transformed using formulae (1) and (2) for the comparison star and observed values in the case of WR 121 (Hiltner & Iriarte 1955). Corresponding standard deviations are listed also.

	V	$V - B$	$B - U$	$U - W$	$B - L$	V_J	$(B - V)_J$
C	-0.212	0.167	0.449	0.188	0.237	7.40	0.392
s.d.	0.003	0.002	0.003	0.004	0.002	0.01	0.005
121	-1.826	0.459	-0.023	0.18	0.065	11.94	1.40
s.d.	0.009	0.010	0.031	0.16	0.021	–	–

(amplitude $0\overset{m}{.}06$). At the bottom of Fig. 1 the V brightness of the comparison star is displayed and found to be very stable indeed (see the standard deviations in Table 3).

The out-of-obscuration observations show a difference between 1989 and 1990. This difference is probably due to the difference in observing strategy (see above). We conclude that WR 121 is stable over a period of a year within $\Delta V = 0.01$, corresponding to $0\overset{m}{.}025$. The observations during normal brightness show a larger scatter from night-to-night than can be expected from the nightly standard deviations. Single WR stars often show such variability. We find as upper limits for the amplitude of variability 0.03 (peak-to-peak) in V and 0.02 in $V - B$, corresponding to $0\overset{m}{.}08$ and $0\overset{m}{.}05$, respectively: this low-amplitude variability emphasizes the magnificence of the event in June 1990.

The light curve in the V-band of the 1990-"eclipse" is displayed in detail in Fig. 7 (Sect. 5); the decline in the first three nights is present in all passbands. Therefore, we suppose that

this was the end of the "ingress". In the following ten days the star recovered from the "eclipse". The depth of this drop in brightness (e.g., half the light in the V-band and more for the bluer bands) can not be caused by emission lines, which we estimate to contribute at most 30 % (equivalent widths from Smith & Aller 1971) and even less in the other bands.

2.1.3. Colour-colour diagrams

The "eclipse" is progressively deeper towards shorter wavelengths ($\Delta V = 0.31$, $\Delta B = 0.40$, $\Delta L = 0.49$, $\Delta U = 0.55$) suggesting that it is caused by extinction. Figs. 2 and 3 show the change of the colours during the 1990 "eclipse" in Walraven colour-colour diagrams. The inserted graphs show the position of the empirical main sequence. The "after-obscuration" values are inserted as a star. WR 121 is highly reddened ($A_{V_J} = 5.2$, van der Hucht et al. 1988). This and the strong emission lines lead to the peculiar position of WR 121 in the colour-colour di-
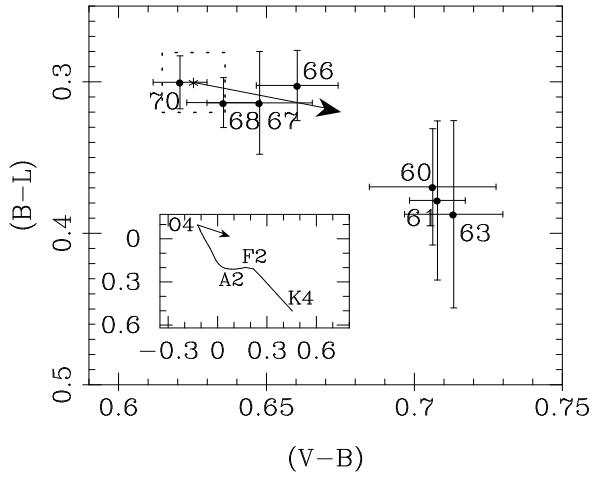
Fig. 2. The $V - B/B - L$ diagram showing the nightly averages during the 1990-"eclipse" of WR 121. The star indicates the average colours and the dotted box shows the mean standard deviation for both axes during normal brightness. The numbers indicate the nights in JD (-2448000) of each data point. The arrow indicates the direction of the interstellar reddening (R=3.1). As a reference, the inset shows the position of the ZAMS in the Walraven system.
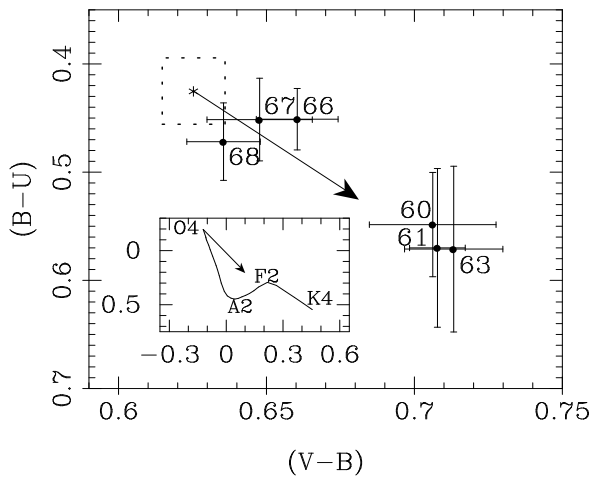

Fig. 3. The same as Fig. 2 but now for $V - B/B - U$.

agrams. The significance of these plots, however, lies not in the exact position of WR 121, but rather in the path followed during the change of brightness. The numbers in Figs. 2 and 3 indicate the Julian date of each data point. The star was reddened by $\Delta(V - B) = 0.08$ at the start of the observations mid-1990. It continued to redden for two more days towards minimum light. After another two more nights the star was already halfway through egress and blueing continued the following nights towards the end of the "eclipse".

This displacement is in the direction of interstellar reddening, indicated by the arrows adopting the reddening law $R = 3.1$. Clearly, the fading of WR 121 can readily be explained by scattering and absorption by dust particles. If this interpretation is
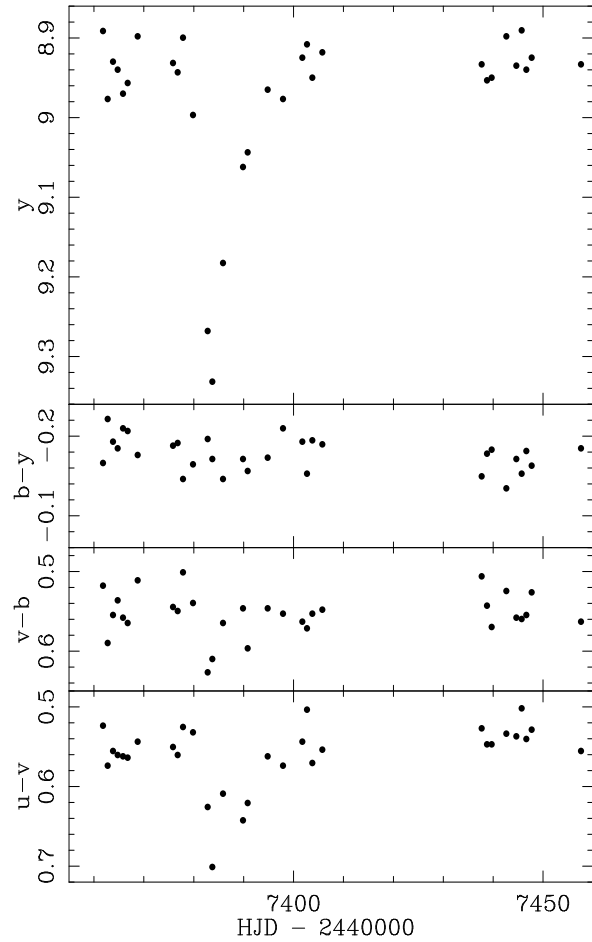

Fig. 4. The LTPV observations of WR 103 around the brightness drop in August 1988. Reddening during the fading is shown in the colour curves. A single deviating point at JD 2447393 has been removed.

true the particles must be circumstellar (Sect. 4) since interstellar extinction cannot change at time scales of days.

2.2. WR 103

To search for another "eclipse" of WR 103 we inspected the $uvby$ data obtained by the Long-Term Photometry of Variables Group (LTPV) (Sterken 1983; Manfroid et al. 1991, 1994; Sterken et al. 1993, 1995).

Indeed, we did find a drop in brightness in August 1988 as shown in Fig. 4, where the y-band observations and the different colours are shown. These values are differential measurements with respect to HD 164152 (B9V). The other comparison star HD 163868(B5Ve) is variable (Sterken & Veen 1997). Because of the shape, depth and colour changes of the "eclipse", this event is easily distinguished from the low-amplitude night-to-night variability (see ref. in Sect. 3.2). The colour changes during this 1988-"eclipse" indicate significant reddening ($\Delta y = 0.^{m}41$, $\Delta b = 0.^{m}43$, $\Delta v = 0.^{m}49$, $\Delta u = 0.^{m}64$). This new "eclipse" of WR 103 displays a completely different

light curve than earlier "eclipses", which we will discuss in the next section.

3. History of occasional "eclipses" of late WC stars

3.1. WR 113

WR 113 (CV Ser, WC8 + O8-9 III-V) is an eclipsing binary *in the classical sense* with a period of 29.704 days (Niemela et al. 1996). The shallow primary eclipses ($\Delta B = 0^{m}05$) are interpeted as atmospheric eclipses when the WR star is in front ($\phi = 0$). There is a slight hint of a secondary minimum (Cherepashchuk 1996). Recently, Niemela et al. (1996) found that the WC8 star has a minimum mass of $14\,M_{\odot}$ and its companion is about twice as massive. Moreover, the system turned out to be eccentric and might even be triple because of the shape of the absorption profiles.

In 1962 the system showed one major drop in brightness (Hjellming & Hiltner 1963), with Strömgren $\Delta y = 0^{m}49$ and $\Delta b = 0^{m}55$. The ascending branch lasted 3 to 4 days. Fig. 10 (Sect. 5) displays the y-band data. Initially, it was considered a primary eclipse until Cowley et al. (1971) found that the event occurred when the companion was in front. These authors suggested that the "eclipse" was due to the occultation of bright material between the two stars. However, as they put forward themselves, the magnitude of the dimming is too large. Moreover, the "eclipses" are not periodic. Only Cherepashchuk (1972) recognised the accidental nature of the "eclipse" and he proposed that ejection of material caused the brightness to drop.

Lipunova (1982) determined more precisely that the minimum occurred at $\phi = 0.560$. Because of its single nature and the orbital inclination in the range $65°–85°$ (Lipunova 1982, Eaton et al. 1985) and probable sizes of both objects, the fading can not be an occultation by the known companion. If a third companion exists (see above), it must have a long period in which case eclipses are highly unlikely.

A second decline in brightness of WR 113 was observed by Williams et al. (1977) in 1976, who observed that the 2.2 μm- and 3.8 μm-magnitude increased by respectively $0^{m}25$ and $0^{m}18$ in four days time ($\phi = 0.54$). Several explanations are discussed by Williams et al. (1977), but all assumed that the phenomenon was periodic. However, subsequent infrared monitoring found the star to be constant at all phases (Williams 1995b). Therefore, we suggest that the infrared "eclipse" in 1976 was similar in nature as the 1962 "eclipse", because of the comparable time scale, its incidence at the same phase, and because of its occasional nature.

3.2. WR 103

Two deep "eclipses" have been reported for the spectroscopic single star WR 103 (WC 9), one in 1909 and another in 1980; a third, shallow one, is presented in Sect. 2.2. The earliest known "eclipse" was uncovered in a study of Harvard Patrol plates by Massey et al. (1984). The shape of this "eclipse" can hardly be established because of the limited accuracy of photographic magnitudes. Still, we conclude that the egress starts rapidly, and then levels off slowly, like the 1988-"eclipse" and the fading of WR 121 (Sect. 2).

The second "eclipse" was observed by Lundström & Stenholm (1982) in 1980 in the $bb'v$ filter system of Smith (1968). The data points (see Fig. 8 in Sect. 5) cover the whole ingress of about 12 days and show an irregularity: the decline hesitates halfway at a depth of about $0^{m}5$, and then continues to drop another $0^{m}7$. If the turn-up of the last data point is real, this egress starts rapidly also. Furthermore, the change in colour during the drop in brightness is small compared to its depth; an upperlimit of ($|\Delta(b - v)| < 0^{m}1$) is determined.

Taking all non-eclipse observations into account, Massey et al. (1984) narrowed the possible periodicity down to 17.7, 35.4, or 70.8 years. The authors find that a cool red supergiant fits the constraints. They note that the presence of such a companion is inconsistent with current evolutionary theory, and that other solutions also encounter severe problems.

Yet another explanation was preferred by Moffat et al. (1986). Based on long-term photometric monitoring a period of 1.75 days is confirmed but not by van Genderen & van der Hucht (1986). This short period is ascribed to a close compact companion and the deep eclipses should then be caused by a precessing disk around the system. If so, a third body (5 to 20 $M_{\odot}$; P of 20 to 60 days) had to be invoked as the motor for the precession.

Each of these models mentioned above may explain the observations. However, the configuration of the alleged companions is very special and the occurrence in the small number of known WR stars has a low probability. Moreover, because of the difference in shape, depth, and colour and the lack of a consistent period the 1988-"eclipse", cannot be another primary eclipse. And, it cannot be a secondary eclipse either because if the primary eclipse is $1^{m}2$, the secondary can only be $0^{m}31$ deep. So. at least for 1988-"eclipse' a new model is required.

4. Circumstellar shells of late WC stars

All three stars that showed occasional "eclipses" (WR 113, WR 103 and WR 121) are of late WC spectral type and have heated dust shells. This is not unusual: Allen et al. (1972) showed that several late-type WC stars have prominent infrared excess. This was attributed to persistent dust shells, which have been investigated by WHT, who performed an infrared survey of most late-type WC and WN stars. Assuming spherical symmetry and a r^{-2}-dependence of the dust density distribution, they derived parameters of the shells of all "dusty" WC stars. Typically, at a few hundred stellar radii dust particles condense (R_c). The height of the dust shell (H) that contributes to the infrared emission can extend out to hundreds of condensation radii.

Even more spectacular is the fact that some WC binaries show a temporary infrared excess (Williams 1995a). Apparently, during a specific phase around periastron the circumstances in the colliding winds give rise to dust formation. The dust is blown away by radiation pressure at almost the wind

Table 4. Properties of the dust shells as determined by WHT: listed are the bolometric flux from the shell and the ratio to the stellar bolometric flux, the inner radius R_c of the dust shell in units of stellar radii, the extent of the cloud H in units of R_c, the temperature T_0 and density ρ_0 at the inner shell edge, the mass of the IR-luminous shell, and the rate at which the dust mass is being replenished.

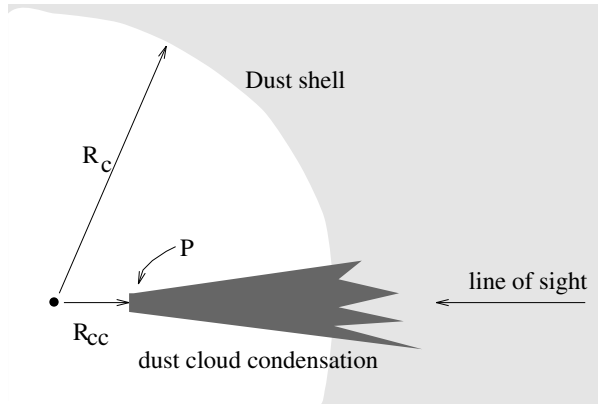| WR	F_{shell} $(10^{-12}$ W m$^{-2})$	$F_{shell}/F_\star$	R_c $(R_\star)$	H (R_c)	T_0 (K)	ρ_0 $(10^{-21}$g cm$^{-3})$	M_{dust} $(10^{-8}$M$_\odot)$	$\dot{M}_{dust}$ $(10^{-9}$M$_\odot$yr$^{-1})$
121	7.3	0.060	180	300	1650	19.0	130.0	17
103	2.1	0.012	220	10	1520	4.0	1.7	5.2
113	11.0	0.011	421	3	1575	1.1	0.9	6.9

Fig. 5. A schematic diagram of a condensing dust cloud causing an "eclipse".

velocity within a few years, as is observed. This confirms the need to replenish the persistent dust shells continuously.

The objects WR 121, WR 103, and WR 113 were included in the survey of WHT and these stars show prominent persistent dust shells, which are among the hottest in the survey. All relevant parameters as determined by WHT are listed in Table 4. The shells around WR 103 and WR 121 have similar inner radii although the one around WR 121 is much more extended and therefore more massive. The shell around WR 113 is also modeled as a spherically symmetric system, although we consider it likely that the dust condensation does not occur spherically symmetric around the system but is localized in the (tail of the) wind-wind interaction cone. And, perhaps because of the small separation, the system acts as a *persistent* dust maker.

The formation of dust particles in the harsh environment of the ionized hot stellar wind is a long-standing theoretical problem, although promising improvements to the theory are suggested (e.g., Cherchneff & Tielens 1995). In the carbon-rich environment and in the absence of hydrogen, the particles consist either of graphite, or amorphous carbon (no emission from SiC is present in the 9.7μm feature). The absence of both the graphite resonance line $\lambda 11.52\mu$m and polycyclic aromatic hydrocarbon feature at $\lambda 11.3\mu$m , is consistent with the supposition that dust is made of amorphous carbon. The size of the particles is determined by the short time a seed particle of 0.003μm can grow in the rapidly expanding stellar wind. They are expected to be smaller than $0.04~\mu$m (WHT).

Generally, the dust shell intercepts only a few percent of the UV starlight and re-emits this in the infrared part of the spectrum. In the case of WR 121, an optical depth of about $\tau_{UV} = 0.06$ is implied if the dust is distributed uniformly over a shell. Therefore, the dust shell contributes marginally to the visual extinction. And indeed, from two studies of the ISM towards WR 121, the extinction towards WR 121 appears to be fully interstellar (Sandford et al. 1995, Figer et al. 1995). The next section will model the fadings we discussed as temporary circumstellar extinction.

5. Modeling the "eclipses" as condensing dust clouds

5.1. Model

We assume that the fading is caused by the formation of a dust cloud in the line-of-sight. As soon as the condensation ends, the star begins to brighten because the dust particles will be blown away very effectively causing the cloud to be diluted. It is assumed that the condensation area is so large as to cover the whole stellar disk immediately (Sect. 6.2.3). Fig. 5 shows a sketch of the situation.

The model parameters are R_{cc}, the distance between the condensing cloud and the star, and P, the "optical depth production". Physically the function P represents the production rate of obscuring material. By introducing this peculiar function P we can model the shape of the obscuration independently of, e.g., the particle size, or the optical parameters of the particles. Also indicated in Fig. 5 is the inner radius R_c of the dust shell, which may be much larger than it is drawn.

The small number of free parameters that we allow turns out to be enough to explain our set of observations and we write:

$$\Delta\tau(t) = \int_{t_c}^{t} P(t) \left(\frac{R_{cc}}{R_{cc} + v_d(t - t_c)} \right)^2 dt \tag{3}$$

and, similarly, after the condensation ceases:

$$\Delta\tau(t) = \int_{t-(t_{me}-t_c)}^{t} P(t) \left(\frac{1}{1 + \frac{v_d}{R_{cc}}(t - t_c)} \right)^2 dt \tag{4}$$

with the condensation starting at t_c, lasting till mid-"eclipse" (t_{me})(see Fig. 8), v_d the dust flow velocity. Since the dust particles condense from the flowing gas, we assume the dust flow velocity to be immediate and constant and equal to the terminal
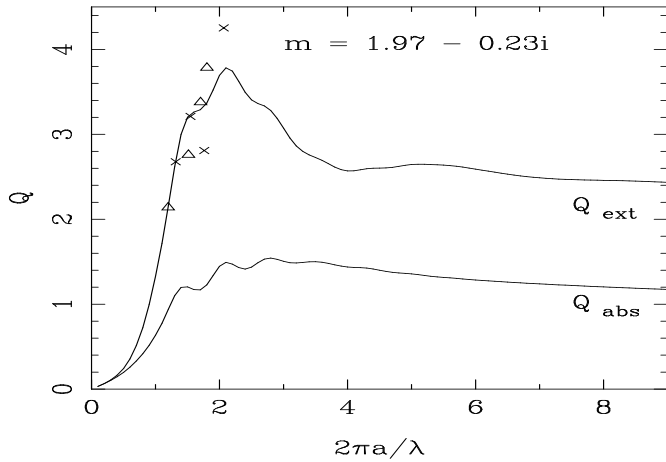
Fig. 6. The extinction and absorption efficiency for a single particle of amorphous carbon (AC-type) with the optical index m as used in the Mie theory. The ratio of observed efficiencies in different passbands as fitted to the curve are plotted, for WR 121 ($\triangle$) and the 1988 event of WR 103 (x).

velocity of the wind (Sect. 6.2.2). Possible acceleration is discussed in Sect. 6.1. We choose to use the terminal velocities as determined by Eenens & Williams (1994) in the infrared. These are systematically about 20 % lower than earlier determinations in the optical. We will use a step function for $P(t)$ equal to P for t between t_c and t_{me} and zero elsewhere. The instantaneous rise to the value P is justified by the rapid ingress. Physically, it is probably due to a high supersaturation of the wind (e.g. Sedlmayr & Gass 1991).

These integrals result in the following description of the ingress:

$$\Delta\tau(t) = P\frac{R_{cc}}{v_\infty}\left[1 - \frac{1}{1 + \frac{v_\infty}{R_{cc}}(t - t_c)}\right] \qquad (t_c < t < t_{me}) \quad (5)$$

and, analogous, for the egress

$$\Delta\tau(t) = \frac{P(t_{me} - t_c)}{(1 + \frac{v_\infty}{R_{cc}}(t - t_c))(1 + \frac{v_\infty}{R_{cc}}(t - t_{me})} \qquad (t_{me} < t). \quad (6)$$

The general features of the obscurations are quite well reproduced by these functions: the ingress that approaches the value PR_{cc}/v_∞ for $t \gg t_c$, which can be interpreted as an equilibrium value where the condensation rate equals the rarefaction of particles flowing out, the asymmetry around mid-"eclipse", the rapid rise in light (or decrease in optical depth) right after mid-"eclipse", and the leveling off later on. If the start time and the time of mid-"eclipse" are well determined, the complete obscuration is fully determined by two parameters P and R_{cc}, since the terminal velocity is defined well enough for our purpose from model atmosphere fits to spectral lines.

We introduced one extra parameter to fit the hesitation during ingress (see Figs. 8 and 10). We assumed that P can be enhanced instantaneously (to be interpreted later, Sect. 6.2.1).

In this view, a burst of condensation starts at t_c at rate P, enhances at time t_d up to P', until it ceases at time t_{me} (see Fig. 8). One easily rewrites the equations with the new integration limits and the two-fold production rate.

We interpret the production rate of optical depth (P) in terms of the dust mass production rate ($\dot{M}_d$), and we write

$$\dot{M}_d = P\frac{\rho}{K} \tag{7}$$

with ρ the mass density of the particles, and, $K = \pi a^2 Q_{ext}/V$ the extinction per unit volume. K is independent of the particle size, when Q depends linearly on a ($a/\lambda < 0.3$).

To derive the physical properties of the dust cloud a particle model is needed. We assume that the particles condense as amorphous carbon, i.e. the same particles that form the permanent circumstellar envelope (see Sect. 4). Rouleau & Martin (1991) have determined the optical constants of different types of amorphous carbon. First, the AC-type (produced by striking an arc between two amorphous carbon electrodes in an argon atmosphere) is quite transparent to optical light. Next, there is a whole group of amorphous carbon material that have a 3 to 4 times higher absorptivity (e.g., produced by burning benzene in air). Perhaps none of these samples represents the soot particles produced in WC winds. However, our best guess is to use the optical constants of the AC-type particles, because they are produced in the absence of hydrogen. Note that Cherchneff & Tielens (1995) pointed out a major difference in pressure and ionization between laboratory circumstances and the WR wind. The mass density of the AC-type amorphous carbon is 1.85 g cm^{-3} (other types of Rouleau & Martin (1991) are in the range from 1.47 to 2.26 g cm^{-3}) and K is 1.4 10^5 cm^{-1}. Additional evidence for such a density comes from the study of meteorites that show small carbon-rich grains, which possibly originate from WR stars, with a density of 1.7 g cm^{-3} (Dorschner & Henning 1995).

5.1.1. Colour changes

In our model the colour differences are due to the wavelength dependence of the extinction. The extinction efficiency for a single particle can be calculated as a function of wavelength using the Mie theory of spherical particles once the optical constants are known. Fig. 6 shows the absorption and extinction efficiency as a function of the particle size over the wavelength, using the AC-type optical constants (Rouleau & Martin 1991); in the wavelength domain of the observations these constants are constant.

To determine the size of the dust particles we need the observations in at least two passbands. First, for a range of particle sizes we calculate the ratio of the efficiency in a particular passband over that of the V-band. Next, the specific particle size is determined by minimizing the differences between the observed and the calculated ratios. Simultaneously, we derive the absolute values for the efficiency. This way we neglect complicating matters like the shape of the passband and the fact that the particles will show a size distribution instead of a single size and

Table 5. Observed obscuration parameters for WR 103, WR 113, WR 121 from the literature and from this study (*)

WR nr	date	$t_{ingress}$ (d)	t_{egress} (d)	pass-band	depth	colour change
103	1909	$\gtrsim 26$	20	m_{pg}	1^m3	—
	1980	$11 - 19$	–	v	1^m2	const.
	1988*	~ 4	10	y	0^m4	red
				u	0^m65	
113	1962	6	3.5	b	0^m55	red
				y	0^m49	
	1976	$\gtrsim 4$	–	2.2μ	0^m27	red
				3.8μ	0^m18	
121	1990*	$\gg 4$	12	V	0^m78	red
				U	1^m38	

are not spherical. Therefore and because of the observational uncertainties, the uncertainty of this determination is large and can probably only be trusted to first order, but the relative results from one obscuration to the other are probably meaningful.

5.2. Model fits

Table 5 summarizes all observational facts of the observed obscurations described above. These display quite large differences from event to event. In a general way this will support the model we present, because condensation is expected to occur at different heights and to last for different periods.

To fit the observations, the magnitude differences with respect to the corresponding out-of-"eclipse" mean were transformed to optical depth differences ($\Delta\tau$). For the Walraven observations of the obscuration of WR 121, the data points were weighted with their standard deviation. Otherwise, equal weights were assigned. The subsequent fitting procedure consisted of trials varying the fixed times (t_c and t_{me} (and t_d)) with steps of 0.05 day. The free parameters were R_{cc} and P (and P'). Only the data points during the obscuration are used in the fitting procedure. The results are listed in Table 6 and will be discussed now.

5.2.1. WR 121

The start of the obscuration of WR 121 in 1990 was not observed (Figs. 1 and 7). However, the parameters are reasonably-well constrained, since R_{cc} is determined mostly by the egress. Using various values of possible times t_{me} the condensation radius ranges from 2 to $4 \cdot 10^{11}$ m, with $v_\infty = 1100$ km s^{-1} (Eenens & Williams 1994). The best fit of the V-band data, weighted by their sigma, results in $R_{cc} = 430$ R$_\odot$. To compare this with the condensation radius of the shell we need the stellar radius. Based on the standard model for WR star atmospheres Howarth & Schmutz (1992) determined a stellar radius of $13 R_\odot$. Then the cloud condensation distance is five times closer than the shell. Note that the standard model is challenged to meet several observational facts indicating that the radius of WR stars is overestimated (Moffat & Marchenko 1996, see also Schaerer
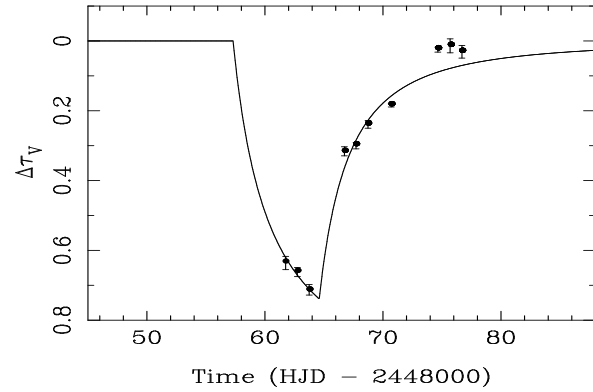
Fig. 7. The ΔV data points from the obscuration of WR 121 in units of optical depth (see Fig. 1 for all data points). The line represents the fit as given in Table 6.
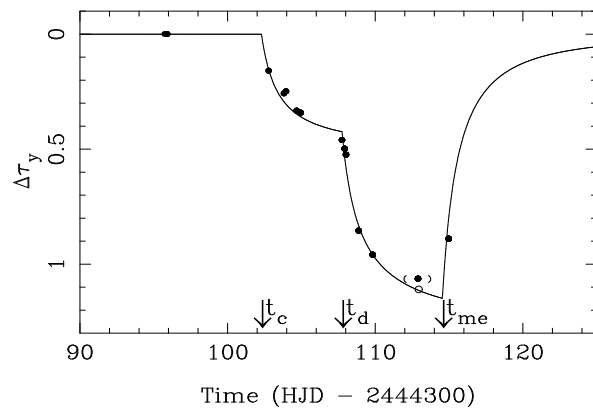
Fig. 8. The data points of the 1980-"eclipse" of WR 103 in optical depth increasing downward. The open circle indicates the position after correction (see text). The line represents the best fit with t_c indicating the start of the condensation, t_d the onset of the higher condensation rate, and t_{me} indicating mid-"eclipse" when the condensation stopped.

1996). However, it is probably not overestimated by a factor five and, therefore, we conclude that the sudden burst of condensation occurs interior to the dust shell.

The optical depth production P varies between 0.3 per day (onset of condensation as early as HJD 2448035) and 0.4 per day (HJD 2448059). If we take the slope of the first three points seriously, the obscuration started quite late, although the ingress might have "hesitated" as in the 1980-"eclipse" of WR 103. This best fit is shown in Fig. 7 and its parameters are listed in Table 6. The production of $P = 0.34$d^{-1} implies a dust mass production rate of $5 \cdot 10^{-10}$kg m^{-2}s^{-1}. The obscuration terminates earlier than the fit indicates. Possibly, other mechanisms, in addition to radial expansion, play a role while diluting or removing the cloud, e.g. non-radial expansion or evaporation of the particles by the hot radiation field.

We match the curve in Fig. 6 for a particle size $a \simeq 0.10\mu$m. The difference between the curve and the observations is even smaller in the Rayleigh scattering domain, e.g. for $a = 0.02\mu$m.

Table 6. Properties of the dust clouds from fitting the time evolution of the obscurations listed in order of increasing R_{cc} and a typical shell. The different times (t_c, t_d and t_{me}) are expressed in HJD - 2400000. Between brackets is indicated the uncertainty in the last digit as follows from the fitting procedure and "f" means that that parameter was held fixed during the fit routine (parameter space was searched for best value, see text). The dust mass production $\dot{M}_{dust}$ (see eq. 7) is in units of (10^{-10} kg m^{-2}s^{-1}).

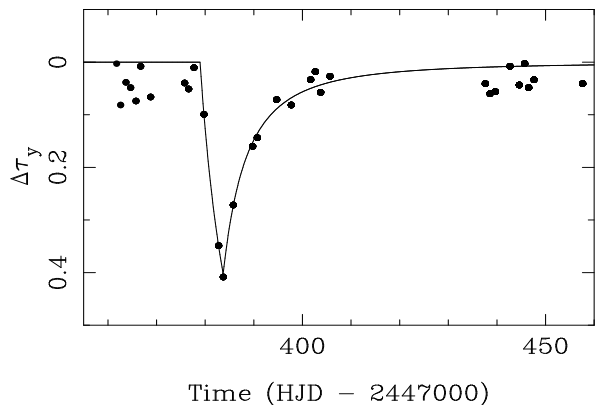| WR	year	t_c	t_d	t_{me}	band	$R_{cc}(R_\odot)$	P(d^{-1})	P'(d^{-1})	$\dot{M}_{dust}$	$a(\mu m)$	Q_{ext}
113	1962	37884.1(1)	37886.50 f	37888.45 f	y	83 f	0.90(4)	1.54(4)	23	0.14	3.4
103	1980	44402.3(1)	44407.75 f	44414.55 f	v	150(10)	0.45(3)	1.19(8)	18	≥ 0.16	2–3
121	1990	48057.3(8)	–	48064.60 f	V	430(10)	0.34(2)		5	0.10	2.1
103	1988	47378.9(2)		47383.70 f	y	1060(110)	0.14(1)		2	0.12	2.6
shell						2500	0.01		0.15	0.01	0.02

Fig. 9. Part of the 1988 season of LTPV-observations of WR 103 observed within filter system 8. One of the possible fits to the points from HJD 2447378 to 2447460 is shown.

Fig. 10. The observations of the 1962-"eclipse" of WR 113 in optical depth with respect to the out-of-"eclipse" mean. The line represents the best fit of a condensing dust cloud from HJD 2437884.0 on.

However, this is only due to the smaller efficiencies causing smaller absolute differences. Since the amount of reddening is not reproduced for the small size, we adopt the larger size.

5.2.2. WR 103

The object WR 103 was not included in the survey by Eenens & Williams (1994). Therefore, we used the WR 121 value $v_\infty = 1100$ km s^{-1}, because both stars are spectroscopically very similar. The fit to the 1909-"eclipse" was troublesome, since the specific times (t_c, t_d, and t_{me}) are not well constrained by the observations. It turns out that equally good fits are obtained for condensation radii between 500 to 1200 R$_\odot$, whether we use a two-fold ingress or not. Therefore, the model results of this obscuration are not used nor listed. We only conclude that the measurements of the 1909-"eclipse" do not disprove the model.

Secondly, the specific times of the 1980 event are reasonably well determined (see Fig. 8). The one data point just before mid-"eclipse" is not very well fitted. However, it turns out that exactly at this point, one of the comparison stars deviates (Lundström & Stenholm 1982). On the assumption that their comparison star C1 changed instead of C2, a correction was applied which shifted the data point satisfactorily towards the fitted curve. Although Massey et al. (1984) rejected the obscuration by dust, because of the absence of a colour change, we point out that
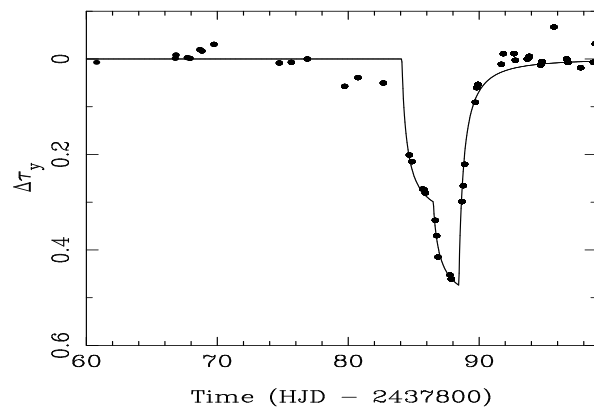
if the particles are large ($a > 0.16$ μm), the extinction will be independent of wavelength.

In the case of the more shallow obscuration in 1988, we arbitrarily used the highest brightness in the y-band after obscuration as zero optical depth (see Fig. 9). The change in colour implies a single particle size of 0.12μm (see Fig. 6). The condensation radius is much larger than for the deep obscurations in 1909 and 1980, because the egress is much slower. The question of periodicity of the *deep* eclipses might have to wait until the year 2050. For now, we prefer the model of a condensing dust cloud to explain the occasional "eclipses" of WR 103.

5.2.3. WR 113

We fitted the 1962 event of WR 113 with the two fold production model with a $v_\infty = 1700$ km s^{-1} (Eenens & Williams 1994). The fit to the b-band data improved considerably when we deleted the measurement for which the simultaneous y-value was discarded already by Hjellming & Hiltner (1963). In the case of WR 113, we fitted both the Strömgren b and the y magnitude and found $R_{cc} = 0.66(6) \cdot 10^{11}$m and $0.50(5) \cdot 10^{11}$m, respectively. We fixed the radius at $0.58 \cdot 10^{11}$m, which yielded practically the same fits. The fitted curve is shown in Fig. 10 and all parameters are listed in Table 6.

The interpretation of the colour changes of this obscuration is more ambiguous than in the case of WR 121, since only two

passbands were used. Those observations can be matched with a cloud of small particles $\sim 0.01\mu$m and equally well for particle sizes from 0.12 to 0.16μm. Larger particles are much more efficient and are thus more likely; therefore, we assume the size to be 0.14(2)μm.

As to the drop in the infrared brightness in 1976, there are too few data points to model this obscuration. However, the change of colour can be interpreted. A perfect match is reached for a particle size of 0.70μm and a very good match is found for 0.06μm. However, no size in between these values can be ruled out. We suppose the particles were bigger than 0.1μm, because otherwise the obscuration in the optical would have been several magnitudes deeper than ever observed. Therefore, we assume the same particle size as for the 1962-"eclipse". In that case the obscuration is as deep at optical wavelength as in 1962.

We derived a cloud condensation distance R_{cc} of $\sim 80\,R_\odot$, which is comparable to the semi-major axis as determined by Massey & Niemela (1981) and Niemela et al. (1996). Moreover, because the phases of the 1962 and 1976 infrared event are practically equal (~ 0.55), we suggest that the clouds are formed in the wind-wind collision zone around the companion. This means that the event was more complex than our model assumes. For example, the dust may not have reached its terminal velocity and may not have flown radially outwards, causing the obscuration to end more rapidly. The question even rises whether only one star was obscured; if so, it would mean that the obscuration of one star happened very effectively and caused twice as much reddening, since both stars are equally bright (Massey & Niemela 1981) (see also Sect. 6.2.1).

6. Discussion

Since the "eclipse" in 1962 of WR 113 one or more ad-hoc explanations have been put forward for each case individually. However, none was ever fully satisfying. We propose that the model of a temporary condensing dust cloud is the answer to these remarkable occasional "eclipses" of "dusty" WR stars. Dust formation has been recognized in those stars long ago. The new aspect of our model is that we assume that the condensation can take place occasionally much closer to the star. However, the concept of a dust cloud obscuring a star is not new at all: it is widely accepted as an explanation for the RCrB star phenomenon.

6.1. RCrB stars and the temperature problem

RCrB stars are wel known for their dramatic drops in brightness (5–9 magnitudes) (O'Keefe 1939, Clayton et al. 1992, Pugach & Skarzhevskii 1993). These events show a rapid ingress of a few days to a low brightness level, which can last for months. Subsequently, the egress starts rapidly and levels off later and within a few days normal brightness is reached. These minima are interpreted as prolonged stages of condensation of carbon-rich dust in the outflowing atmosphere in the line of sight. Both the ingress and the egress are remarkably similar to those of the WC stars. Though these stars are very different from WR stars:

Table 7. Different type of stars that show eclipse-like events due to formation of dust clouds. The rather cool RCrB stars hardly suffer any mass loss unless dust is being formed.

object	type	T_{eff} (kK)	$log(\dot{M})$ ($M_\odot$/yr)	v_∞ (km/s)	ref.
RCrB	RCrB	7			
V348 Sgr	?	20	-6.5	190	[a]
CPD-56°8032	[WC11]	30–34	-5.5	225–240	[b]
WR 121	WC9	29	-4.4	1100	[c]

[a]   Hamann 1996
[b]   Crowther et al. 1996, Hamann 1996, Leuenhagen 1996
[c]   Howarth & Schmutz 1992

they are F and G supergiants ($< 1M_\odot$). Their radius is of the order of $100\,R_\odot$, and the temperature is typically 7000 K. Therefore, the wind is also cooler and mostly neutral, even showing many molecules. More general information on RCrB stars can be found in an observational overview by Cottrell (1996).

This RCrB star phenomenon is studied intensively, but not yet completely understood. Observations indicate that the condensation takes place at 2–5 stellar radii. Theory, however, does not predict dust formation before the gas is out to 10–15 stellar radii, because the temperature would be too high. So, even for these cool stars the temperature is a problem.

Recently, so called *hot* RCrB stars, like MV Sgr and DY Cen with temperatures up to 20000 K are identified; these have very rare minima (Pollaco & Hill 1991). Similar photometric behaviour is also discovered for the [WC11]-star CPD-56°8032 (Pollacco et al. 1992; Lawson& Jones 1996), possibly due to a phase of dust formation. Furtermore, the curious object V348 Sgr may be an object in between the RCrB and [WC11] stars. It shows huge drops of brightness (6 magnitudes) due to the formation of dust clouds on a time scale of days to months (Heck et al. 1985).

Table 7 lists several parameters for each of these very different objects, that show obscurations due to circumstellar dust. What they have in common is a hot, massive outflow which is hydrogen deficient and carbon rich. Still, each group of stars is a unique laboratory with their specific carbon abundance, temperature and density to study the phenomenon of dust condensation.

Clearly, the temperature is a problem for all types of hot stars that show dust cloud "eclipses". Moreover, for WR stars it is not our model that raises this problem but the observation of the infrared excess in the first place, because no model so far has explained the formation of any dust particle anywhere around a WC star, also not in the shell.

Having said so, we will discuss the problem for our model specifically. To quantify the discrepancy we calculated the temperature of a dust particle in radiative equilibrium to be about 5000 K (Eq. 6 by WHT) at the distance where the clouds condense (parameters of WR 121). Though dust condensation is believed to occur only *far below* the evaporation temperature (<2000 K).

Answering this criticism of our model, we point out that this temperature argument considers a stationary situation while condensation events or "eclipses" are dynamic by definition. Furthermore, perhaps evaporation does occur causing the obscuration to end faster. In that case our model underestimates the distance of the clouds, which in turn alleviates the temperature problem. Still the temperature problem remains to be solved.

A recent observation by Crowther (1997) might contribute to the solution of the temperature problem of WC stars. He observed WR 104 (WC9) spectroscopically to be about one magnitude fainter and to show a completely different spectrum that, amongst other changes, shifted to lower ionization. Apparently, the temperature in the line forming region dropped and simultaneously the star faded one magnitude. Conclusions need to await full analysis of this object and its spectral change, but if a fading event always coincides with such a temperature drop the problem is much alleviated.

6.1.1. Shocks: a possible mechanism of seed formation?

A very important step with regard to the theory of dust formation in stellar winds is presented by Woitke et al. (1996a,b). These authors describe a mechanism for RCrB stars that allows much lower temperatures at 1.5–3 stellar radii as the observations indicate. In short, the pulsation of the star causes an outrunning shock in the atmosphere, which heats the wind locally to a high temperature; the excess of energy is radiated away quickly and subsequent re-expansion of a local element in the atmosphere causes adiabatic cooling. In particular cases, a gas temperature below that of the radiative equilibrium can be reached. Woitke et al. (1996b) point out that this mechanism will not only work for pulsating stars, but for every case where a strong shock will hit an atmospheric element with the appropriate density.

We suggest that this mechanism might also be the clue to the riddle of dust formation around WR stars in general and the formation of clouds as we described. On the basis of the X-ray luminosity of WR stars shocks are believed to permeate the stellar wind and may be the consequence of the instability of the radiative driven WR winds (Gayley & Owocki 1995). Time resolved spectroscopy and spectro-polarimetry reveal so-called "blobs" in the wind, which might be identified with the shocks. In that case it is noteworthy that WR 103 was amongst the stars with the largest line variability of a sample of 9 stars in the study by Moffat & Robert (1992) (see also Lépine et al. 1996). Additional indication that dust formation is related to shocks, is given by the episodic dust makers (Sect. 4). These long-period colliding-wind binaries show a phase of dust formation around periastron when the collision of the winds is most severe, causing strong shocks.

Our suggestion that the mechanism discussed above is applicable to dust formation around WR stars, sheds new light on the model that we applied. If the dust particles condense in a dense, low-velocity post-shock environment, the dilution of the cloud is then not properly described by a smooth radial expansion at $v = v_\infty$, but merely by the acceleration after the shock

has passed. That may well change our determinations of R_{cc}, which in turn might alleviate the temperature problem also.

6.2. Interpretation of the model

We are aware that the full problem of dust formation in WR winds involves the physics and chemistry of the gas-to-solid phase transition, including radiative hydrodynamics. However, we consider the simplicity of the model that we presented and the good predictions it makes very appealing. We will address several features that need some discussion.

6.2.1. The two-fold ingress: "hesitating" light curves

In the case of WR 113, the two-fold ingress might be a consequence of its binarity. One could imagine that a cloud covers one of the stars and by expansion covers the second one somewhat later, causing a two-step ingress. However, at the phase of the "eclipse" the projected distance is only a few stellar radii, so it may be unrelated to its binary nature. Moreover, WR 103, a spectroscopic single star, showed a similar behaviour and such irregularities are also known to occur at RCrB stars.

For a single star one may think of a few mechanisms to cause a two-fold ingress. Possibly, additional matter flows to the condensation area in the line of sight to enhance the condensation rate suddenly, which is the situation that we modelled. But other scenarios are possible, like a neighbouring cloud expanding non-radial into the line of sight, or a second clouds begins to condense in the shade of the first cloud because the heating dropped locally by 30 %, or more. These latter scenarios should be modelled using more parameters, like a second condensation radius. We did not try additional free parameters, because the fits were satisfying.

It is noteworthy that the colour from the first to the second burst changes for both stars. This may indicate that the size of the particles differ from the first to the second burst. However, because of the shape of the extinction efficiency curve, this interpretation is not unique. For example, in the case of the 1962-event of WR 113, reddening increases from the first to the second burst, which might be due to the growth of the particles from about 0.07 μm to 0.14 μm, or a *decrease* from 0.15 μm to 0.12 μm. More multi-colour observations with full coverage of the obscuration are needed to interpret the two-fold ingress properly.

6.2.2. The dust flow velocity

One of the assumptions to derive the distances of the clouds is that the dust flow velocity is equal to v_∞. However, the distances we derive turn out to be so small that the wind may not have reached its terminal velocity yet (Moffat 1996). If the flow velocity is lower, the distance must be even shorter to produce an effective dilution.

Besides the higher temperature close to the star, the higher radiation pressure is a problem also. Since the drag force can only balance that pressure at a dust drift velocity of $\sim$

100 km s^{-1} relative to the wind. At such a speed the particles may not survive the collisions with the ions. However, since the particles turn out to be much larger and, therefore, more massive than in the dust shell (Sect. 4), the acceleration is less effective than WHT derive and they may not reach such high differential velocities during an obscuration.

6.2.3. The size and mass of a typical cloud and the number of clouds

From the depth of the obscuration we can infer a lower limit to the size of the cloud assuming the optical depth to be infinite. For example, when an obscuration is one magnitude deep, the cloud must cover at least 60 % of the stellar disk during mid-"eclipse". However, since most obscurations show reddening, we can safely assume that the cloud is not opaque and covers the whole disk of the star. Because more parameters would be necessary, we did not consider whether full coverage is reached only after expansion of the cloud. An upper limit to the size of the clouds cannot be determined and the condensation might occur all around the star. This would influence the model results in the sense that the extinction efficiency would decrease, since scattered light from the whole sphere would contribute to the received flux (Greenberg & Wang 1972, Voshchinnikov & Karjukin 1994).

Awaiting further study, we assume that the clouds are as large as the continuum- and line-forming region of the WC9 star. Assuming a radius of $13\,\mathrm{R}_\odot$ (WR 121; Howarth & Schmutz 1992) and a condensation time of 4 days, we deduce the mass of the whole cloud to be of the order 10^{16} kg. This is only a small fraction (10^{-4}) of the total dust mass produced by WR 121 during that time (WHT). However, the fraction of the local wind mass that condenses into dust is the same from the innermost cloud to the shell. This leads us to suggest that the cloud condensation and the shell formation are similar phenomena, the only difference being that the cloud condensation occurs much closer to the star. This could mean that the shell is not homogeneous, but that it consists of many optically-thin distant clouds.

From the small number of obscurations, we conclude that events of the magnitude as we have seen here occur quite rarely. To quantify this statement, we counted published observations of each program star versus the number of observed obscurations. Table 8 lists all references with a significant number of spectroscopic and photometric observations of the three program stars. Because of gaps within an observing run, the period over which an obscuration can be excluded is in most cases at least twice the amount of actual observing nights.

To infer a recurrence time scale from this mixed data set is dangerous. The time scale might differ from star to star and depend on the depth of the obscuration. However, the order of magnitude can be established on the basis of these numbers. The recurrence time is definitely longer than one month and probably longer than one year. On the other hand, one obscuration per century would mean that we have been very lucky to get so many observations of obscurations. Therefore, the recurrence time scale is likely of the order of one decade (3–30 years).

Table 8. The number of observing nights (N) for the three stars that showed occasional obscurations. The number of obscurations is listed in column 2.

WR	#	N	reference
103	3	31	Isserstedt & Moffat 1981
		16	Lundström & Stenholm 1982
		> 700	Massey et al. 1984 (plates)
		39	Moffat et al. 1986
		62	van Genderen & van der Hucht 1986 and other Walraven phot.
		140	LTPV 1983-1993
113	2	28	Hiltner (1945)
		26	Hjellming & Hiltner 1963
		27	Kuhi & Schweizer 1970
		39	Cowley et al. 1971
		20	Morrison & Wolff 1972
		79	Cherepashchuk 1972
		116	Schild & Liller
		6	Williams et al. 1977 (IR)
		50	Massey & Niemela 1981
		43	Lipunova 1982
		6	Eaton et al. 1985 (UV)
		2615	Cherepashchuk 1996
121	1	60	this paper

A recurrence time scale of one decade is also consistent with the fact that these dust obscurations have not been observed for other "dusty" WR stars (yet). More obscurations of other "dusty" WC stars may be present in archives. Note, however, that the search by Schild & Liller (1975) of 116 Harvard patrol plates for "eclipses" of WR 113 was fruitless and Massey et al. (1984) investigated more than 700 plates to find only one "eclipse".

The number of clouds condensing all around a "dusty" WR star is derived as follows. Assuming that every 5 years all positions on the sky of the WR star have been covered by a cloud at a typical condensation distance, $R_{\rm cc} = 250\,\mathrm{R}_\odot$ and with a size equal to the disk of the star, we estimate that such a condensation takes place every week. This would mean that there are always a few of these clouds present between the star and the shell, of which only a small fraction occurs in the line of sight.

6.2.4. Condensation rate and particle size dependent on distance?

From the observations we note that "eclipses" with small changes of colour show a rapid egress. In the model we presented, this translates to the tendency for the particles to be larger if the condensation occurs closer to the star (Table 6). For the one object for which two occasional obscurations are observed in two passbands, WR 103, this correlation is clearly present. Taking WR 113 and WR 121 into account this trend remains and inclusion of the shell confirms the trend (Sect. 4). This might not be too surprising since large particles can survive higher temperatures because they are more efficient at cooling.

In Table 6 another trend is discernible between the production rate of optical depth and the distance to the cloud. Smaller R_{cc} values are connected with higher P values. Or, in terms of direct observables: the deeper the obscuration, the "faster" the egress. With Eq. 7, this means a higher dust mass production rate closer to the star. Also this correlation holds out to the shell, since in the shell hardly any optical depth is produced.

On the one hand both correlations can be understood as the consequence of higher wind densities for smaller distances from the star: more seed particles are formed and the particles can grow larger. But, on the other hand, the higher temperatures closer to the star counteract both the formation of seed and the growth rate strongly. So, this needs confirmation and further study.

7. Conclusions

The essential conclusion is that occasional "eclipses" of late-type WC stars are related to their production of dust. These objects and [WC 11]-stars may be hot star counterparts of RCrB stars. Since WR stellar winds are permeated by shocks, the mechanism of a "cooling trap" after a shock, which is supposed to create seeds around RCrB stars, may also play a role in WR winds.

We present a specific model that fits all known occasional non-periodic obscurations of "dusty" WC stars (WR 103, WR 121 and WR 113). They are interpreted as obscurations by clouds in the line of sight, in which dust particles condense before they are dispersed by the radiation pressure. The cloud condensation occurs at a distance between ∼10 to ∼100 stellar radii. This is interior to the circumstellar dust shell (∼100 to ∼1000 stellar radii, WHT). At these short distances the temperature of a dust particle in equilibrium with the radiation field is much too high. This remains a severe problem for our model, though note the spectral change of WR 104 during an eclipse (Crowther 1997).

We found two trends that may be real: both the size of the dust grains and the mass condensation rate increase for decreasing distance of the condensing cloud to the star. This can be interpreted, quite naturally, as a consequence of the increasing wind density coming closer to the star, although the temperature counteracts severely.

In order to study the formation of dust particles in hot WR winds a photometric multi-colour monitoring campaign of all 25 "dusty" WR stars is called for, with the possibility to take spectra when an obscuration occurs. If this phenomenon is a general feature of "dusty" WR stars, a few obscurations may be caught within a year. Moreover, dust as a possible cause of any kind of variability of these stars, cannot be ignored any longer.

We have given a viable explanation for the "eclipse" of WR 121 and a solution for the "curious case" of WR 103 and for WR 113, the star that was once believed to have stopped eclipsing.

References

Allen D.A., Harvey P.M., Swings J.P., 1972, A&A 20, 333
Cherchneff I., Tielens A.G.G.M., 1995, in: K.A. van der Hucht, P.M. Williams (eds) Wolf-Rayet stars: Binaries, Colliding Winds, Evolution. IAU Symp. No. 163, Kluwer, Dordrecht, p. 346
Cherepashchuk A.M., 1972, Sov. Astron. 15, 955
Cherepashchuk A.M., 1996, in: J.-M. Vreux, D. Fraipont-Caro, *et al.* (eds.), Wolf-Rayet Stars in the Framework of Stellar Evolution, *Proc. 33rd Liège Int. Asptroph. Coll.* (Liège: Univ. of Liège), p. 155
Clayton G.C., Whitney B.A., Stanford S.A., Drilling J.S., 1992, ApJ 397, 652
Cottrell P.L., 1996, in: C.S. Jeffery & U. Heber (eds), Hydrogen-Deficient Stars, ASP Conf. Ser. 96, p.127
Cowley A.P., Hiltner W.A., Berry C., 1971, A&A 11, 407
Crowther P.A., 1997, MNRAS, submitted
Crowther P.A., De Marco O., Storey P.J. et al. 1996, in: C.S. Jeffery & U. Heber (eds), Hydrogen-Deficient Stars, ASP Conf. Ser. 96, p.149
Dorschner J., Henning Th., 1995, A&AR 6, 271
Eaton J.A., Cherepashchuk A.M., Khaliullin Kh.F., 1985, ApJ 296, 222
Eenens P.R.J., Williams P.M., 1992, MNRAS 255, 227
Eenens P.R.J., Williams P.M., 1994, MNRAS 269, 1082
Feinstein A., 1974, AJ 79, 1290
Figer D.F., McLean I.S., Morris M., 1995, ApJ 447, L29
Gayley K.G., Owocki S.P., 1995, ApJ 446, 801
van Genderen A.M., van der Hucht K.A., 1986, A&A 162, 109
Greenberg J.M., Wang R.T., 1972, Mem. Soc. Roy. Liège 6 ser 3, 197
Hamann W.-R., 1996, in: C.S. Jeffery & U. Heber (eds), Hydrogen-Deficient Stars, ASP Conf. Ser. 96, p.127
Heck A., Houziaux L., Manfroid J., 1985, A&AS 61, 375
Hiltner W.A., 1945, ApJ 102, 492
Hiltner W.A., Iriarte B., 1955, ApJ 121, 556
Hjellming R.M., Hiltner W.A., 1963, ApJ 137, 1080
Howarth I.D., Schmutz W., 1992, A&A 261, 503
van der Hucht K.A., 1992, A&AR 4, 123
van der Hucht K.A., Hidayat B., Admiranto A.G. et al., 1988, A&A 199, 207
van der Hucht K.A., Conti P.S., Lundström I, Stenholm B., 1981, Space Sci. Rev 28, 227
Isserstedt J., Moffat A.F.J., 1981, A&A 96, 133
Koesterke L., Hamann W.-R., 1995, A&A 299, 503
Kuhi L.V., Schweizer F., 1970, ApJ 160, L185
Lawson W.A., Jones A.F., 1996, in: C.S. Jeffery & U. Heber (eds), Hydrogen-Deficient Stars, ASP Conf. Ser. 96, p.151
Lépine S., Moffat A.F.J., Henriksen R.N., 1996, ApJ 466, 392
Leuenhagen U., 1996, in: C.S. Jeffery & U. Heber (eds), Hydrogen-Deficient Stars, ASP Conf. Ser. 96, p.150
Lipunova N.A., 1982, Sov. Astron. Lett. 8, 128
Lub J., Pel J.W., 1977, A&A 54, 137
Lundström I., Stenholm B., 1982, in: C.W.H De Loore, A.J. Willis (eds), Wolf-Rayet Stars: Observations, Physics, and Evolution, IUA Symp. No. 99, Reidel, Dordrecht, p. 289

Lundström I., Stenholm B., 1984, A&AS 58, 163
Manfroid J., Sterken C., Bruch A. et al., 1991, AAS 87, 481
Manfroid J., Sterken C., Cumow B. et al., 1994, AAS 109, 329
Massey P., Niemela V.S., 1981, ApJ 245, 195
Massey P., Lundström I., Stenholm B., 1984, PASP 96, 618
Mathis J.S., Cohen D., Finley J.P., Krautter J., 1995, ApJ 449, 320
Merrill P.W., Burwell C.G., 1950, ApJ 112, 72
Moffat A.F.J., 1996, in: J.-M. Vreux, D. Fraipont-Caro, *et al.* (eds.), Wolf-Rayet Stars in the Framework of Stellar Evolution, *Proc. 33rd Liège Int. Asptroph. Coll.* (Liège: Univ. of Liège) p. 199
Moffat A.F.J., Marchenko S.V., 1996, A&A 305, L29
Moffat A.F.J., Robert C., 1992, in: L. Drissen, C. Leitherer, A. Nota (eds.) Non-isotropic and Variable Outflow from Stars, ASP Conf. Ser. 22, 203
Moffat A.F.J., Lamontagne R., Cerruti M.A., 1986, PASP 98, 1170
Moffat A.F.J., Shara M.M., 1986, AJ 92, 952
Morrison N.D., Wolff S.C., 1972, PASP 84, 635
Niemela V.S., Morrell N., Barbá R., Bosch G., 1996, Rev. Mex. Astron. Astrofis. Serie Conf. 5, 100
O'Keefe J.A., 1939, ApJ 90, 294
Pel J.W., 1986, Internal Report, Leiden Obs.
Pollacco D.L., Hill P.W., 1991, MNRAS 248, 582
Pollacco D.L., Kilkenny D., Marang F., 1992, MNRAS 256, 669
Pugach A.F., Skarzhevskii V.O., 1993, AZh 70, 327 (=Astron. Rep. 37, 169)
Rouleau F., Martin P.G., 1991, ApJ 377, 526
Sandford S.A., Pendleton Y.J., Allamandola L.J., 1995, ApJ 440, 697
Schaerer D., 1996, A&A 309, 129
Schild R., Liller W., 1975, ApJ 199, 432
Schmidt G.D., 1988, in: G.V. Coyne et al.(eds), Polarized radiation of circumstellar origin, Vatican Observatory, Vatican City State, p. 641
Smith L.F., Aller L.H., 1971, ApJ 164, 275
Smith L.F., Hummer D.G., 1988, MNRAS 230, 511
Schulte-Ladbeck R.E., 1994, Ap&SS 221, 347
Sedlmayr E., Gass H., 1991, in: K.A van der Hucht, B. Hidayat (eds), Wolf-Rayet stars and their interrelations with other massive stars in galaxies, IAU Symp. No. 143, Kluwer, Dordrecht, p. 335
Smith L.F., 1968, MNRAS 140, 409
Smith L.F., Shara M.M., Moffat A.F.J., 1990, ApJ 358, 229
Sterken C., 1983, ESO Messenger 33, 10
Sterken C., Manfroid J., Anton K. et al., 1993, AAS 102, 79
Sterken C., Manfroid J., Beelen D. et al., 1995, AAS 113, 31
Sterken C., Veen, P.M., 1997, IBVS, in preparation
Torres A.V., 1988, ApJ 325, 759
Torres A.V., Massey P., 1987, ApJSS 65, 459
Voshchinnikov N.V., Karjukin V.V., 1994, A&A 288, 883
Williams P.M., 1995a, in: K.A. van der Hucht, P.M. Williams (eds) Wolf-Rayet stars: Binaries, Colliding Winds, Evolution, IAU Symp. No. 163 Kluwer, Dordrecht, p. 335
Williams P.M., 1995b, discussion on paper by P.M. Williams, in: K.A. van der Hucht, P.M. Williams (eds), Wolf-Rayet stars: Binaries, Colliding Winds, Evolution, IAU Symp. No. 163, Kluwer, Dordrecht, p. 345
Williams P.M., Beattie D.H., Stewart J.M., 1977, Observatory 97, 76
Williams P.M., van der Hucht K.A., Thé P.S., 1987, A&A 182, 91 (WHT)
Woitke P., Krüger D., Sedlmayr E., 1996a, A&A 311, 927
Woitke P., Goeres A., Sedlmayr E., 1996b, A&A 313, 217

Note added in proof: The HIPPARCOS-satellite (The Hipparcos Catalogue, ESA 1997, ESA SP-1200) observed another eclipse of WR 121 in 1991. The accompanying figure (Fig. 11) shows the data points around eclipse that were not discarded by either of the reduction consortia nor influenced by an interfering object in either field of view. Note that the limiting magnitude of system (λ_{max} = 452 nm) is about 12^{m}4. This event is in accordance with the concept of our model.
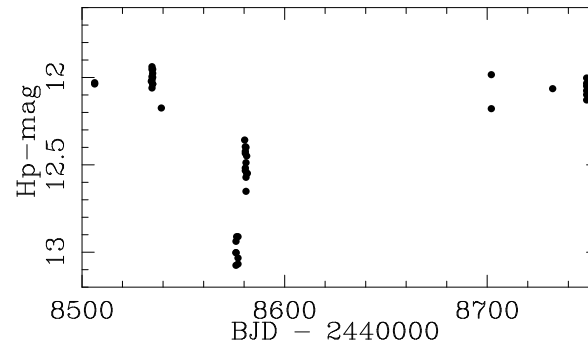

Fig. 11.